Electrodeposition of Ag and Pd on a Reconstructed Au(111) Electrode Surface Studied by *In situ* Scanning Tunneling Microscopy

Satoru Takakusagi,[1+] Ken Kitamura[1] and Kohei Uosaki[1,2,3]*

[1]*Physical Chemistry Laboratory, Division of Chemistry, Graduate School of Science, Hokkaido University, Sapporo 060-0810, JAPAN,* [2]*International Center for Materials Nanoarchitectonics Satellite (MANA),National Institute of Material Science (NIMS), Sapporo 060-0810, JAPAN,* [3]*ISE member*

Abstract Electrochemical deposition of Ag and potential-induced structural change of the deposited Ag layer on a $23\times\sqrt{3}$ reconstructed surface of Au(111) electrode were followed by *in situ* scanning tunneling microscope (STM). A uniform Ag monolayer was formed on a reconstructed Au(111) surface in a 50 mM H_2SO_4 solution at +0.3 V (vs. Ag/AgCl) after adding a solution containing Ag_2SO_4 so that the concentration of Ag^+ in the STM cell became ca. 2 μM. No characteristic height corrugation such as the Au reconstruction was observed on the surface, indicating that the lifting of the substrate Au reconstruction occurred by Ag deposition. The formed Ag monolayer was converted to a net-like shaped Ag nano-pattern of biatomic height when the potential was stepped from +0.3 V to –0.2 V in the solution containing 2 μM Ag^+. This result indicates that the substrate Au(111)-(1×1) surface was converted to the reconstructed surface even in the presence of Ag adlayer. Quite different structure was observed for Pd deposition on a reconstructed surface of Au(111) electrode at +0.3 V and the origin for this difference between Ag and Pd deposition are discussed.

Keywords: Ag, Pd, Au(111), electrodeposition, surface reconstruction, STM

*Corresponding author: Kohei Uosaki

TEL:+81-11-706-3812 FAX: +81-11-706-3440 e-mail: uosaki@pcl.sci.hokudai.ac.jp

[+]Present address: Catalysis Research Center, Hokkaido University, *Sapporo 001-0021, JAPAN*

1. Introduction

Electrochemical deposition of Ag on Au(111) electrode surface is a good model system to study the morphology of the deposited layer because the interaction and the lattice misfit between a metal deposit and a substrate is very strong and negligibly small (0.4 %), respectively [1-16] and has been studied by a wide variety of techniques, including scanning tunneling microscopy (STM) [1,2,5,8,9,14,16], atomic force microscopy (AFM) [3,4,6], second harmonic generation (SHG) spectroscopy [13], quartz crystal microbalance (QCM) [7], X-ray diffraction [11,12] and extended X-ray absorption fine structure (EXAFS) [10]. In particular underpotential deposition (UPD) of Ag has received special attention and the structures of adsorbates, both metal and anion, and their dependencies on the potential and electrolyte composition have been well studied [2-6]. It has been reported that UPD Ag layer of various coverage up to two monolayer is formed depending on the electrode potential [14,15]. Reports on the overpotential deposition (OPD) of Ag on a Au(111) surface are, however, very limited [9, 14]. A layer-by-layer growth was observed at the initial stage of OPD up to 10 monolayers at low overpotentials [14]. Both for UPD and OPD of Ag, a Au(111) electrode is generally kept at a potential much more positive than the Ag deposition potential and then scanned negatively or stepped to a potential more negative than the Ag deposition potential. Since the initial potential is actually positive enough to lift the reconstruction of Au(111) surface, Ag deposition usually takes place on a Au(111)-(1x1) surface.

In our previous paper [17], we reported the first *in situ* real time monitoring of potentiostatic electrodeposition of Ag on a $23\times\sqrt{3}$ reconstructed Au(111) surface using electrochemical STM and discussed the effect of the uniformly spaced inhomogeneous sites of the Au reconstruction on the morphology of the electrodeposited Ag adlayer. A solution containing Ag^+ was added into an STM cell filled with H_2SO_4 solution while keeping the potential of the Au(111) electrode more negative than the potential of reconstruction lifting in

electrolyte so that the Ag deposition was initiated. It was found that while Ag of biatomic height was nucleated on a faulted hcp region of the reconstruction and grew preferentially along the hcp lines (the $<11\bar{2}>$ directions), resulting in a line shape at –0.2 V (vs. Ag/AgCl), monatomic Ag was preferentially deposited in a hcp domain and also formed a line shape at +0.3 V [17]. These results showed that both substrate surface structure and electrode potential were important for determining the growth mode and morphology of the Ag adlayer.

In the present study, we investigated further the growth of Ag and Pd adlayer on a reconstructed surface of Au(111) electrode using *in situ* STM. The formation of a uniform Ag monolayer on a Au(111) surface at +0.3 V was confirmed and drastic morphology change of the Ag adlayer by the potential step from +0.3 V to –0.2 V, leading to the formation of a complex nanopattern with a net-like shape of biatomic height, was observed. This result indicates that the substrate Au(111)-(1×1) surface was converted to the reconstructed surface even in the presence of Ag adlayer. Quite different structure was observed for Pd deposition on a reconstructed surface of Au(111) electrode at +0.3 V and the origin for this difference between Ag and Pd deposition are discussed.

2. Experimental

2.1. Materials. A (111) facet on a single crystal bead of Au, which was prepared by the Clavilier's method [18], was used as a substrate for the STM measurements. Electrolyte solutions were prepared using H_2SO_4 (Suprapure reagent grade, Wako Pure Chemicals), Ag_2SO_4(Reagent grade, Wako Pure Chemicals), K_2PdCl_4 (Reagent grade, Wako Pure Chemicals), and Milli-Q water.

2.2. Electrochemical STM Measurements. In situ electrochemical STM measurements were carried out using a homemade electrochemical STM cell, which can accommodate the single-crystal electrode. STM images were recorded in a constant current mode using a NanoScope E (Digital Instruments). An Au/AuO_x and a platinum wire were used as a

quasi-reference and a counter electrode, respectively. The electrolyte solution was deaerated by passing purified argon gas for at least 20 min before being introduced into the STM cell. Electrochemical potentials of the Au(111) substrate (E_s) and STM tip (E_t) were independently controlled by a bipotentiostat (Digital Instruments). All potentials were quoted with respect to Ag/AgCl in the present study. STM tips were mechanically cut Pt/Ir wire (80/20, φ=0.3 mm) insulated with Apiezon wax. The single crystal electrode was annealed with hydrogen flame just before each measurement and was mounted to the STM cell after cooling in air. 50 mM H_2SO_4 solution was then introduced into the cell while controlling the electrode potential at a preset value.

3. Results and Discussion

3.1. Ag deposition on a Reconstructed Au(111) surface

3.1.1. Formation of UPD Monolayer on a Reconstructed Au(111) surface

It is well known that the potential induced reversible lifting and restoration of surface reconstruction of Au(111) electrode take place around +0.35 V vs. Ag/AgCl in a sulfuric acid solution [19-23]. Figure 1 (a) shows a typical STM image of Au(111) surface in 50 mM H_2SO_4 electrolyte measured at +0.3 V (vs. Ag/AgCl). A characteristic feature of a herringbone structure of $23\times\sqrt{3}$ reconstructed surface was observed, confirming of the presence of the reconstructed phase.

Figure 1(b) is an STM image of the Au(111) surface at +0.3 V obtained 24 min after the addition of 2 μl of 1 mM Ag_2SO_4 + 50 mM H_2SO_4 solution to the STM cell so that the concentration of Ag^+ became ca. 2 μM (ca. 1 μM Ag_2SO_4 + 50 mM H_2SO_4 in the STM cell). We have already studied the deposition process of Ag on a $23\times\sqrt{3}$ reconstructed Au(111) surface at this potential (+0.3 V) in our previous paper [18], and reported that the nucleation and growth of monatomic Ag took place preferentially in the hcp region of the reconstruction, forming a line shape along the $<11\bar{2}>$ directions, followed by the much slower growth along

the perpendicular directions (the <1$\bar{1}$0> directions). Fig 1(b) confirmed the previous results.

As shown in Figure 1(c), a very uniform surface without any prominent height corrugation such as the reconstruction was observed more than 1 h after the Ag^+ addition. Since the reversible potential for Ag/Ag^+ in 2 μM Ag^+ solution is calculated to be +0.26 V vs. Ag/AgCl, the electrode potential (+ 0.3 V) was more positive than the reversible potential by +0.04 V, i.e., in UPD region where formation of a uniform monolayer of Ag on a Au(111)-(1x1) surface is expected [14,15]. The STM image of Fig. 1(c) indicated that the UPD monolayer of Ag was formed on the Au(111)-(1x1) surface, suggesting that the deposition of the Ag monolayer lifted the reconstruction of the underlying Au(111) to the (1x1) structure.

3.1.2. Formation of a Net-like Shaped Nano-pattern of Ag bilayer Induced by Substrate Surface Restructuring

The structural conversion of the Ag monolayer formed on the Au(111)-(1x1) surface at +0.3 V upon potential step from +0.3 V to –0.2 V was investigated. In our previous paper, we have reported that the line shaped Ag deposits of biatomic height on the reconstructed Au(111) surface at -0.2 V were converted to the monatomic islands by stepping the potential to +0.3 V while the underlying reconstruction of Au(111) kept unchanged by the potential step [20]. Figure 2 shows the sequentially obtained STM images of the Au(111) surface in ca. 1 μM Ag_2SO_4+50 mM H_2SO_4 after keeping the potential at -0.3 V for more than 1 h. Figure 2(a) shows the surface before the potential step. As observed in Fig. 1(c), a very uniform surface was observed, confirming the formation of monatomic Ag layer on Au(111)-(1x1) surface. The electrode potential was stepped at the lower part of Figure 2(b). Shortly after the potential step, Ag islands with a globular or particle shape of biatomic height were formed as more clearly seen in Figure 2(d), which is a zoomed image of the white rectangular area of Fig. 2(b). A complex two-dimensional pattern was then developed and, finally, the whole surface was covered with the net-like pattern as shown in Figure 2 (c), which was recorded 5

min 50 s after the potential step. Cross sectional analysis along the line A-B in Fig. 2(c) revealed that the height of the pattern was 0.47 ± 0.02 nm, corresponding to biatomic height of Ag. The structure of this pattern as clearly shown in Fig. 2(e), which is a zoomed image of the white rectangular area of Fig. 2(c), is very similar to the one observed at the initial stage of Ag deposition at -0.2 V [17], suggesting the restoration of the $23 \times \sqrt{3}$ reconstructed Au(111) surface. Figure 2(f) is an STM image of different location on the surface obtained 21 min after the potential step. The surface structure is very similar to the one of Fig. 2(c), showing that the net-like structure was stable and no further Ag deposition took place, although there existed Ag^+ ion in the solution and the potential was in OPD region. In our previous paper, we reported the Ag multilayer deposition at -0.2 V [17]. It must be noted, however, that while the concentration Ag^+ in the STM cell was 160 μM for the multilayer deposition, it was only 2 μM in this case and the rate of OPD should be very small due to the slow diffusion of Ag^+ ion.

The schematic model for the potential induced structural conversion of the uniform Ag monolayer to the net-like pattern of biatomic height upon potential step from +0.3 V to –0.2 V is shown in Figure 3. The monatomic Ag layer, which was formed on the Au(111)-(1x1) surface at +0.3 V, was first converted to the Ag islands with a globular or particle shape of biatomic height immediately after the potential step because biatomic Ag layer is more favored than monatomic Ag layer at –0.2 V as already suggested in the previous paper [20]. The islands then grew not uniformly but to form the complex net-like pattern. The formation of the complex net-like pattern seems to be induced by the reconstruction of the Au(111) surface to the $23 \times \sqrt{3}$ structure with herringbone pattern, which is a slow process. It is interesting to note that the underlying Au(111)-(1×1) was converted to the reconstructed Au surface by the potential step even in the presence of Ag monolayer because the adlayer usually stabilizes the (1×1) surface of the substrate. The partial exposure of the Au substrate by Ag bilayer formation and small deposition rate of Ag may be the origin of the

surface restructuring of the substrate Au(111).

3.2. Pd deposition on a Reconstructed Au(111) Surface

Electrochemical deposition of Pd from $PdCl_4^{2-}$ in acidic solution usually takes place on a Au(111)-(1x1) surface as is the case of Ag deposition from Ag^+ because the deposition potential is more positive than +0.35 V. We have already reported that electrodeposition of Pd from $PdCl_4^{2-}$ solution on a Au(111)-(1x1) surface proceeded two-dimensionally (2D) with an epitaxial layer-by-layer growth mode based on *in situ* STM, QCM and SXS study of Pd deposition [24-27]. Both overpotential depositions of Pd [24] and Ag [14] result in epitaxial layer for over 10 ML, showing the deposition behavior of Pd and Ag on Au(111)-(1x1) are similar. Thus, the comparing of Pd and Ag deposition on a reconstructed Au(111) surface should be interesting.

Figure 4(a) and (b) show *in situ* STM images of Au(111) electrode surface at +0.3 V in 50 mM H_2SO_4 solution 65 min and 285 min after adding 20 μl of 1mM K_2PdCl_4 + 50 mM H_2SO_4, respectively. The concentration of $PdCl_4^{2-}$ in the STM cell was ca. 20 μM. As shown in Fig. 4 (a), preferential nucleation and growth of Pd took place at the bending point of the double bright lines of the reconstruction, i.e., "elbow site". More closer inspection of the image indicates that the growth of Pd tends to occur preferentially at the fcc domain. A previous study in ultra-high vacuum (UHV) also showed that the Pd islands nucleated at the "elbow site" of the herringbone structure of the reconstructed Au(111) surface [28]. According to recent calculation, the in-plane nearest-neighbor atomic distance of the Au reconstruction surface is shorter by 3~7 % in the region of the discommensuration lines (bridge site) including the elbow sites and by 2% in the hcp region than that in the fcc region, where the surface atoms are nearly in registry with the bulk lattice (2.86 Å) [29]. These results indicate that the defective regions such as elbow sites are favored as nucleation sites because the local surface mismatch between Pd and Au in the defective regions is smaller than that in the other regions.

The heights of the Pd islands in Fig. 4(a) and (b) are in the range of 0.2~0.7 nm, which correspond to one to three atomic heights of Pd, suggesting three-dimensional (3D) growth of the Pd layer. This is in contrast to those observed in Fig. 2, where 2D growth of Ag on a reconstructed Au(111) surface was observed. Since surface tensions of Ag ($\gamma_{Ag} = 1.3$ J/m^2) and Pd ($\gamma_{Pd} = 2.0$ J/m^2) are smaller and larger, respectively, than that of Au ($\gamma_{Au} = 1.5$ J/m^2), 2D and 3D growth modes are expected for Ag and Pd, respectively [30, 31].

4. Conclusion

A uniform Ag monolayer was confirmed to form on a Au(111) electrode surface in a 50 mM H_2SO_4 solution at +0.3 V, where the surface was of the $23\times\sqrt{3}$ reconstructed structure, when a solution containing 1 mM Ag_2SO_4 and 50 mM H_2SO_4 was added to the STM cell so that the concentration of Ag^+ was ca. 2 μM followed by keeping more than 30 min. Upon potential step from +0.3 V to -0.2 V, the uniform Ag monolayer formed was converted first to Ag islands with a globular or particle shape of biatomic height then to a complex nanopattern with a net-like shape, possibly induced by slow development of $23\times\sqrt{3}$ reconstructed structure on the Au(111) surface at -0.2 V. The present and previous [20] results indicate that the complex structure of Ag adlayer can be formed on a Au(111) electrode by controlling the potential and the Ag^+ concentration precisely. Pd deposition on a reconstructed Au(111) surface at +0.3 V was found to proceed in 3D growth mode after preferential nucleation at the elbow sites of the Au reconstruction. The origin of this difference from Ag deposition mode was discussed.

5. Acknowledgments

The present work was partially supported by the Grant-in-Aid for Scientific Research (A) (No. 18205016) and for Young Scientists (B) (No.19750102) and World Premier

International Research Center (WPI) Initiative on Materials Nanoarchitectonics (MANA) from the Ministry of Education, Culture, Sports, Science and Technology, Japan.

References

[1] T. Hachiya, K. Itaya, *Ultramicroscopy* **42** (1992) 445.

[2] K. Ogaki, K. Itaya, *Electrochim. Acta* **40** (1995**)** 1249.

[3] C.H. Chen, S.M. Vesecky, A. Gewirth, *J. Am. Chem. Soc.* **14** (1992**)** 451.

[4] P. Mrozek, Y. E. Sung, M. Han, M. Gamboa-Aldeco, A. Wieckowski, C.H. Chen, A. Gewirth, *Electrochim. Acta* **40** (1995**)** 17.

[5] S. Garcia, D. Salinas, C. Mayer, E. Schmidt, G. Staikov, W.J. Lorenz, *Electrochim. Acta* **43** (1998**)** 3007.

[6] P. Mrozek, Y.E. Sung, A. Wieckowski, *Surf. Sci.* **335** (1995**)** 44.

[7] H. Uchida, M. Miura, M. Watanabe, *J. Electroanal. Chem.* **386** (1995**)** 261.

[8] S.G. Corcoran, G.S. Chakarova, K. Sieradzki, *J. Electroanal. Chem.* **377** (1994) 85.

[9] S.G. Corcoran, G.S. Chakarova, K. Sieradzki, *Phys. Rev. Lett.* **71** (1993**)** 1585.

[10] J. H. White, M. J. Albarelli, H.D. Abruna, L. Blum, O.R. Merloy, M.G. Samant, G.L. Borges, J.G. Gordon, *J. Phys. Chem.* **92** (1988) 4432.

[11] E.D. Chabala, A.R. Ramadan, T. Brunt, T. Rayment, *J. Electroanal. Chem.* **412** (1996) 67.

[12] A. R. Ramadan, E. D. Chabala, T. Rayment, *Phys. Chem. Chem. Phys.* **1** (1999**)** 1591.

[13] D.A. Koos, G.L. Richmond, *J. Phys. Chem.* **96** (1992**)** 3770.

[14] M. J. Esplandiu, M.A. Schneeweiss, D.M. Kolb, *Phys. Chem. Chem. Phys.* **1** (1999) 4847.

[15] T. Kondo, J. Morita, M. Okamura, T. Saito, K. Uosaki, *J. Electroanal. Chem.* **532** (2002) 201.

[16] D. Borissov, R. Tsekov, W. Freyland, *J. Phys. Chem. B* **110** (2006**)** 15905.

[17] S. Takakusagi, K. Kitamura, K. Uosaki, *J. Phys. Chem. C* **112** (2008**)** 3073.

[18] J. Clavilier, R. Faure, G. Guinet, R. Durand, *J. Electroanal. Chem*. **107** (1980**)** 205.

[19] H. Honbo, S. Sugawara, K. Itaya, *Anal. Chem.* **62** (1990**)** 2424.

[20] A. Cuesta, M. Kleinert, D. M. Kolb, *Phys. Chem. Chem. Phys*. **2** (2000) 5684.

[21] D.M. Kolb *Prog. Surf. Sci*. **51** (1996) 109.

[22] O.M. Magnussen, J. Hageböck, J. Hotlos, R.J. Behm, *Faraday Discuss*. **94** (1992) 329.

[23] T. Kondo, J. Morita, K. Hanaoka, S. Takakusagi, K. Tamura, M. Takahasi, J. Mizuki, K. Uosaki, *J. Phys. Chem. C* **111** (2007**)** 13197.

[24] H. Naohara, S. Ye, K. Uosaki, *J. Phys. Chem. B* **102** (1998) 4366.

[25] H. Naohara, S. Ye, K. Uosaki, *Colloids and Surf. A* **154** (1999) 201.

[26] M. Takahasi, Y. Hayasi, J. Mizuki, K. Tamura, T. Kondo, H. Naohara, K. Uosaki, *Surf. Sci.* **461** (2000) 213.

[27] M. E. Quayum, S. Ye, K. Uosaki, *J. Electroanal. Chem.* **520** (2002) 126.

[28] C. J. Baddeley, R. M. Ormerod, A. W. Stephenson, R. M. Lambert, *J. Phys. Chem*. **99** (1995) 5146.

[29] H. Bulou, C. Goyhenex, *Phys. Rev. B* **65** (2002) 045407.

[30] H. Heinz, R. A. Vaia, B. L. Farmer, R. R. Naik, *J. Phys. Chem. C* **112** (2008) 17281.

[31] W. R. Tyson, W. A. Miller, *Surf. Sci.* **62** (1977) 267.

[32] However the above discussion considering surface tension does not explain why electrochemical deposition of Pd proceeds with an epitaxial layer-by-layer growth mode on a Au(111)-(1x1). In our previous paper on electrodeposition of Pd on Au(111)-(1x1), we proposed that the $PdCl_4^{2-}$ adlayer with an ordered structure of $\sqrt{7} \times \sqrt{7}$ R19.1 on a deposited Pd island inhibits the vertical but favors lateral, i.e., 2D growth of Pd.[24,25] In the present case, the adsorbed $PdCl_4^{2-}$ layer might not have an ordered structure because Pd island nucleated on the defective region such as elbow sites is expected not to have an uniform internal structure, i.e., different interatomic distance and different height of the Pd atoms. This may promote the reduction of $PdCl_4^{2-}$ and growth of Pd on the terrace of the Pd island, resulting in 3D growth of Pd layer.

Figure captions

Figure 1

In situ STM images (80×80 nm^2) of Au(111) electrode surface at +0.3 V in (a) 50 mM H_2SO_4 solution. (b) and (c) were obtained 24 min and more than 1 h, respectively, after adding 2 μl of 1mM Ag_2SO_4 + 50 mM H_2SO_4 to the STM cell (cell volume, ca. 1 ml). E_{tip} = 0.35 V, I_{tip} = 3.0 nA. The images (a), (b) and (c) observed the different region of the sample surface.

Figure 2

In situ STM image (285×285 nm^2) of the Au(111) electrode obtained in ca. 1 μM Ag_2SO_4+50 mM H_2SO_4 after keeping the potential at +0.3 V for more than 1 h (a). Potential was stepped to –0.2 V at the lower part of (b) as indicated by an arrow and (c) was recorded 5 min 50 s after the potential step. The height profile along the line A-B is also shown in (c). Zoomed images (51×243 nm^2) of the white rectangular areas in (b) and (c) are shown as (d) and (e), respectively. (f) was recorded 21 min after the potential step (280×280 nm^2). E_{tip} = 0.35 V, I_{tip} =3.0 nA.

Figure 3

Schematic model for the structural conversion of the uniform monatomic Ag layer to the net-like biatomic pattern induced by the potential step from +0.3 V to –0.2 V.

Figure 4

In situ STM images of Au(111) electrode surface at +0.3 V in 50 mM H_2SO_4 (a) 65 min and (b) 285 min after adding 20 μl of 1mM K_2PdCl_4 + 50 mM H_2SO_4 to the STM cell (volume: ca. 1 ml) . E_{tip} = 0.55 V, I_{tip} = 3.0 nA. Image size (a) 90×90 nm^2, (b) 150×150 nm^2.

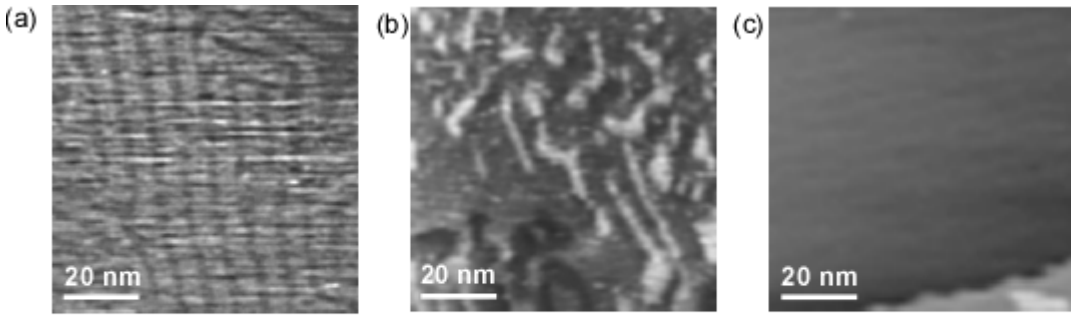

Fig. 1 Takakusagi et al.

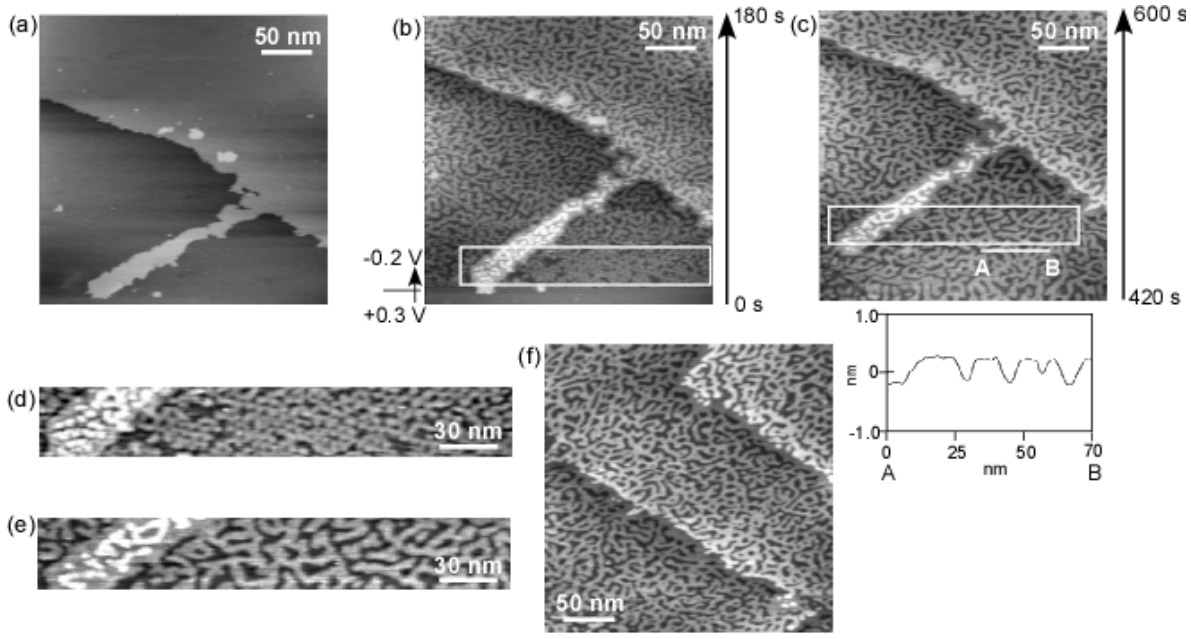

Fig. 2 Takakusagi et al

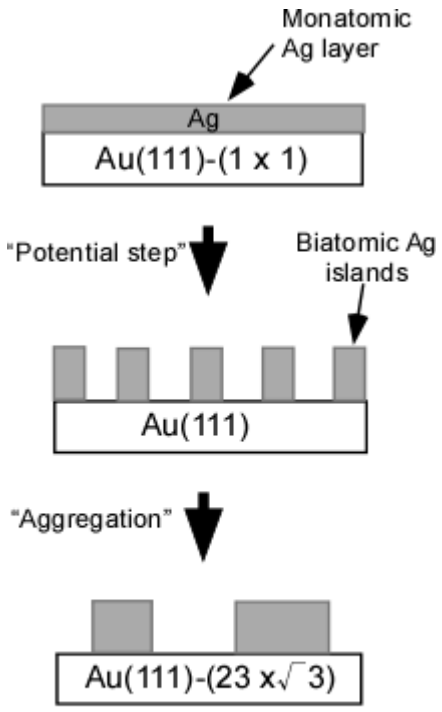

Fig. 3 Takakusagi et al

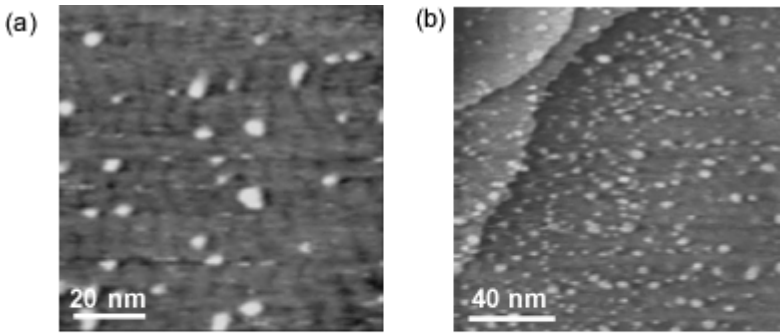

Fig. 4 Takakusagi et al